A&A manuscript no.
(will be inserted by hand later)

Your thesaurus codes are:
11.01.1, 11.05.2, 11.19.5, 11.05.1, 11.19.2

ASTRONOMY
AND
ASTROPHYSICS
1.2.2008

Metallicity indicators across the spectrum of composite stellar populations

C. S. Möller, U. Fritze - v. Alvensleben, K. J. Fricke

Universitätssternwarte, Geismarlandstr. 11, D - 37083 Göttingen, Germany

Received 28 December 1995, accepted 10 June 1996

Abstract. With a chemically consistent evolutionary synthesis approach we follow the enrichment of individual chemical elements in the ISM. We describe the time evolution of broad band colors U to K and metal indices (Fe5335, Fe5270, Mg_2, Mgb), taking into account the increasing initial metallicities of successive generations of stars. Using specific star formation prescriptions for the different spectral types of galaxies, we show our model galaxy broad band colors, synthetic spectra, and ISM abundances are in agreement with observations of nearby samples and template galaxies of the respective spectral types.

We compare our synthetic Mg_2 indices with observations and study the time evolution of the stellar index [MgFe] for composite elliptical galaxy models and for simple stellar populations of various metallicities. We show how the luminosity weighted stellar metallicity indicators in different wavelength bands from U to K compare to each other for the various star formation histories and how they evolve in time. We analyse as a function of wavelength the luminosity contributions of stellar subpopulations with different metallicities in the various galaxy types. The relations between luminosity weighted stellar metallicity indicators in different passbands, stellar absorption indices and ISM abundances are shown to depend significantly on the star formation history and evolutionary stage.

Key words: Galaxies: abundances; evolution; stellar content; elliptical; spiral.

1. Introduction

Strong efforts have been devoted to calibrate and intercompare stellar metallicity indicators determined for galaxies in various wavelength regimes, e.g. in the NIR where the indices are less age dependent than in the optical wavelength range. Many of the problems arising in this context have to do with the fact that galaxies are complex stellar systems containing subpopulations of various ages and metallicities. The relative light contributions of these different subpopulations can not only depend on the star formation (SF) history of the galaxy but also on the wavelength range of interest. The majority of stars in galaxies have metallicities about solar or lower. Only in the bulges of spirals and in the central regions of giant ellipticals may subpopulations of stars with metal abundances reaching a few times solar be present. Arimoto & Yoshii (1986) presented a first attempt to explore the effect of the continous enrichment of the successive stellar generations on the photometric evolution of composite stellar populations. Our chemically consistent model follows both the spectral evolution of successive stellar generations, which may have different metallicities, and the chemical enrichment of the ISM.

Another well-known problem is the age-metallicity-degeneracy (e.g. O'Connell 1976, Bica & Alloin 1986, Bica et al. 1988, Faber et al. 1995). A lot of effort has been made to disentangle this degeneracy by measuring stellar metal indices in different stellar systems (Burstein et al. 1984, Bica & Alloin 1987 ff), and recently for a set of individual stars covering a wide range in metallicity, effective temperature and surface gravity (Gorgas et al. 1993). Bica (1988), Worthey (1994), Worthey et al. (1994), Bressan et al. (1995) use these varous libraries of metal indices for modelling the indices of composite stellar populations. Until now, calibrations of theoretical indices were taken mainly from single burst populations or star clusters.

In this paper we show the time evolution of some indices commonly used for galaxies with different star formation histories taking into account in a consistent way, the evolution of the initial metallicity for successive stellar generations.

The present paper is organized as follows: in Sec. 2 we describe our chemically consistent evolutionary code and in Sec. 3 we present the comparison of our results with observational data. In Sec. 4 we analyse the wavelength dependence of the luminosity weighted stellar metallicities and in Sec. 5 we discuss the relations between stellar

Send offprint requests to: Claudia S. Möller

indices and gas metallicity for galaxies of various spectral types. Sec. 6 summarizes our conclusions.

2. The Evolutionary Synthesis Model

2.1. Computational method

Our model is basically a synthesis of a photometric evolutionary code, similar to Bruzual & Charlot (1993), and a chemical evolution scheme for ISM abundances described by Matteucci et al. (1991 ff).

The initial condition is a homogeneous gas cloud of a given mass and primordial metallicity $Z = 10^{-8}$ (closed box 1 - zone model, instantaneous mixing). The total stellar mass, gas content and abundances are calculated by integrating Tinsley's equations (e.g. Tinsley 1972). Supernova I contributions to [Fe/H] from carbon deflation of white dwarfs in binary systems are taken into account in the way described by Matteucci & Tornambè (1987) and Matteucci et al. (1991).

Our model follows the chemical enrichment of a series of individual elements in the ISM as well as the metallicity evolution of the stellar population, together with its spectral evolution. The evolution of each star is followed in the HR diagram from birth to its final phases so that at each timestep the distribution of all stars over the HRD is known (Fritze - v. Alvensleben 1989, Krüger et al. 1995). This HRD population is used to compute the integrated colors in two different ways. At any given timestep an integrated galaxy spectrum is synthesized from our library of stellar spectra. This library is chosen from stellar atmosphere models (Kurucz 1992) for the five metallicities [Fe/H]= -2.5, -1.5, -0.5, -0.3, 0.3. With tabulated filter characteristics for UBVRIJHKL bands, spectrophotometric colors can be deduced from the synthetic galaxy spectrum (see also Guiderdoni & Rocca - Volmerange 1987). We also derive the integrated colors of the galaxy population from photometric calibrations (UBVRI: Green et al. 1987, V-K: Taylor et al. 1987) as a function of effective temperature T_{eff} and luminosity class LC for all stellar evolutionary tracks. The agreement between both methods is better than 0.1 mag if emission lines from the ISM are excluded.

In the **chemically consistent model** the evolution of the HRD population is followed with the five sets of stellar tracks for five different metallicities ($Z = 10^{-4}, 10^{-3}, 4 \times 10^{-3}, 10^{-2}, 4 \times 10^{-2}$) compiled by Einsel et al. (1995). We distinguish five discrete metallicity ranges, one for each set of stellar tracks. If the ISM metallicity increases above one of our limiting metallicities, the evolution of stars formed thereafter are followed with the tracks for the higher metallicity. The HRD population is calculated for each metallicity together with the appropriate photometric color calibration. The total galaxy luminosities (U to K) at any given timestep are obtained by coadding the various single metallicity contributions. Synthesizing the galaxy spectra is done by summing the stellar spectra, weighted by the distribution of the HRD population.

Our computational code follows the distribution of stellar populations over the five discrete metallicity regimes and calculates their respective luminosity contributions in specific wavelength regimes (Möller 1995).

2.2. Input physics

We use detailed stellar evolutionary tracks for the five metallicities $Z = 10^{-4}, 10^{-3}, 4 \times 10^{-3}, 10^{-2}, 4 \times 10^{-2}$ to follow the metal enrichment of the stellar population. These tracks include all important stages from the main sequence to core helium exhaustion or AGB (onset of thermal pulses) and were calculated from various authors. These sets of stellar tracks were compiled and first used by Einsel (1992), who devoted much effort in selecting from the vast literature those tracks, which are as consistent as possible with the physical assumptions. These sets altogether comprise 170 stellar tracks with 2882 HRD - states. Stars with metallicities higher than twice solar are not included in our model, however their contribution to the global spectral properties of normal galaxies is negligible. The colors have been calibrated with Green et al. (1987) color tables. Linear interpolation has been done in the physical variables log g, T_{eff}, and Z of these tables, to attach UBVRI-colors to each of the discrete points of our stellar evolutionary tracks in the HRD. The temperature range of the tables reaches up to 20 000 K, above which colors fortunately become almost metallicity independent. (V-K) has been calibrated with Bessel & Brett (1988) tables, excepted for the red giants where we use the table by Taylor et al. (1987). Einsel et al. (1995) give a detailed description of these tracks and the sources from which they were taken.

The basic parameters for this type of evolutionary model are the initial mass function (IMF) and the SF law. The IMF is taken from Scalo (1986) in the form $\phi(m) \sim m^{1+x}$ with indices x=0.25, 1.35 and 1.70 between the limits 0.15$M_\odot$, 1$M_\odot$, 2$M_\odot$, 60$M_\odot$, respectively. We take into account the dark matter in normalizing the IMF to the fraction of visible mass FVM = 0.5 (Bahcall et al. 1992).

Following Sandage (1986) we describe the various spectrophotometric galaxy types with specific star formation rates (cf. Table 1). Besides these galaxy types (=Hubble types), we calculate simple stellar populations (SSPs) for different metallicities which form stars only in an initial burst within the first $3 \cdot 10^8$ yr. The SSPs are a useful description of star clusters and any SF history of a galaxy can be described in terms of a series of SSPs. This is already shown by Bica (1988), who takes into account for the first time, the full spread in metallicity.

The calculation of stellar lifetimes, yields and remnants are described in detail in Fritze - v. Alvensleben & Gerhard (1994). A detailed description of the chemical evo-

Table 1. Star formation rates $\psi(t)$ and characteristic timescales for star formation t_*. $g := \frac{M_G}{M_{tot}}$ for various galaxy types.

Type	SFR(t) [$M_\odot$/ yr]	t_* [Gyr]
E	$1.2 \cdot 10^{-9} M_{tot} \cdot e^{-t/t_*}$	1.0
S0	$4 \cdot 10^{-10} g$	2.2
Sa	$3 \cdot 10^{-10} g$	3.0
Sb	$2 \cdot 10^{-10} g$	5.0
Sc	$1 \cdot 10^{-10} g$	9.0
Sd	$0.6 \cdot 10^{-10} M_{tot}$	10.5

lution model for individual ISM element abundances (e.g. ^{24}Mg, ^{56}Fe) which we use for our index calibrations are also given there.

We assign the stellar indices Mg_2, Mgb, Fe5335 and Fe5270 to all evolutionary stages of the five sets of stellar tracks using the empirical fitting functions of Gorgas et al. (1993). For each stellar population we synthesize the indices from the individual values of all their stars, weighting by their respective luminosity at the wavelength of the index. We also analyse the [MgFe] (Bressan et al. 1995) index, which is the geometric mean of the two indices Mgb and $\langle Fe \rangle$, [MgFe] = (Mgb $\langle Fe \rangle)^{0.5}$ where the index $\langle Fe \rangle$ is the mean of the indices Fe5270 and Fe5335 ($\langle Fe \rangle$ = (Fe5270 + Fe5335)/2). The global indices for model galaxies and SSPs at any time are calculated by summing the stellar indices for each stellar evolutionary stage, weighted by the total light contribution in the V band of all the stars at this position in the HRD.

The galaxy spectra are computed by a superposition of stellar atmosphere spectra from Kurucz (1992) weighted by the number of stars present in each spectral type and luminosity class. We use a library with 264 stellar spectra altogether, 44 for each metallicity, covering the range 3500 K to 47500 K, which corresponds to spectral types from M3 to O5, and log g = 0.5 to 5.0. For $T_{eff} \leq$ 3500K we supplement this library with observed spectra (M4V, M6V) of solar metallicity from the UV (Wu et al. 1983) to the optical (Gunn & Stryker 1983) and adding a black body spectra in the IR.

3. Model Galaxies and Comparison with Observation

To visualize the metallicity effects on the color evolution, we plot in Fig. 1 the chemically consistent model, together with three single metallicity models ($Z = 10^{-4}, 4 \cdot 10^{-3}, 4 \cdot 10^{-2}$) and their evolution in time. To justify the use of our SF laws (Tab. 1) together with our Scalo IMF for the different spectral types, we show that the chemically consistent calculations reproduce the color observations from de Vaucouleurs et al. (1991 RC3) of typical ellipticals (top), Sb - spirals (middle) and Sd - galaxies (bottom panel). As expected, the color evolution at constant metallicity for all Hubble types is bluer at lower metallicities. It is clear that models with tracks of solar metallicity are redder than our chemically consistent model and that this difference is even more pronounced at earlier times. In our E - model the color evolution starts, of course, from the lowest metallicity, reaching the curve for $Z = 4 \cdot 10^{-3}$ after ∼4 Gyr and keeping this color until 15 Gyr. The mean stellar metallicity stays subsolar throughout a Hubble time. In Sb-type galaxies after 8 Gyr, the (B-V) curve for the chemically consistent model approaches the one that only uses evolutionary tracks with $Z = 4 \cdot 10^{-3}$. Because of their constant star formation rate Sd - galaxies evolve very slowly towards redder colors. The chemically consistent (B-V) color of Sd's only reaches that of a single metallicity population with $Z = 4 \cdot 10^{-3}$ after 11 Gyr.

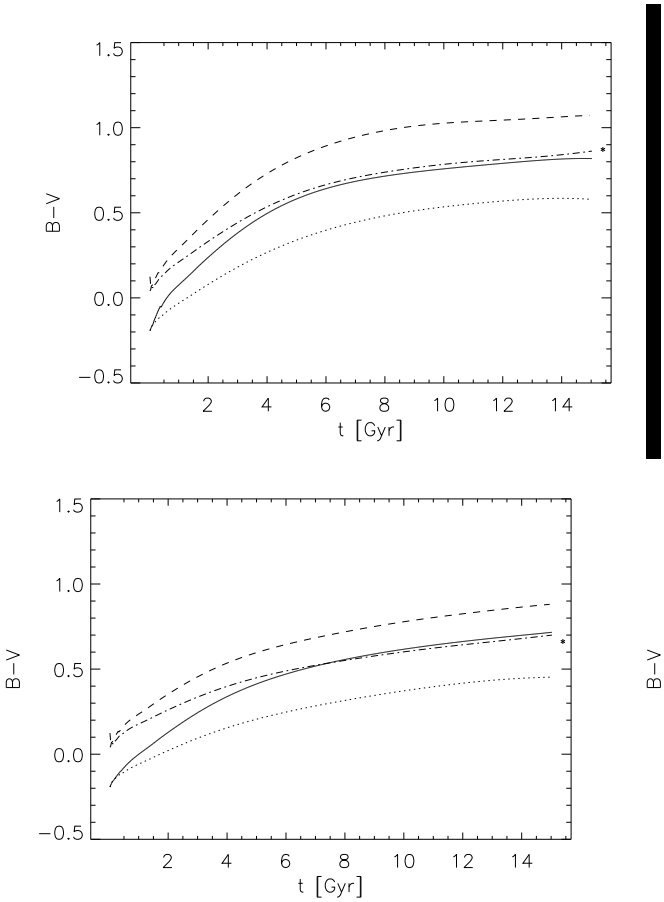

Fig. 1. Color evolution (B-V) of different spectral types: elliptical (top panel), Sb (middle panel) and Sd (bottom panel). Lines are solid for the chemically consistent model, dotted for $Z = 10^{-4}$, dash - dotted for $Z = 4 \cdot 10^{-3}$ and dashed for $Z = 2Z\odot$. The data points (*) are the observations from de Vaucouleurs et al. (1991 RC3).

In calculations with a single constant metallicity, stellar tracks with $Z = 4 \cdot 10^{-3}$ seem to produce colors in bet-

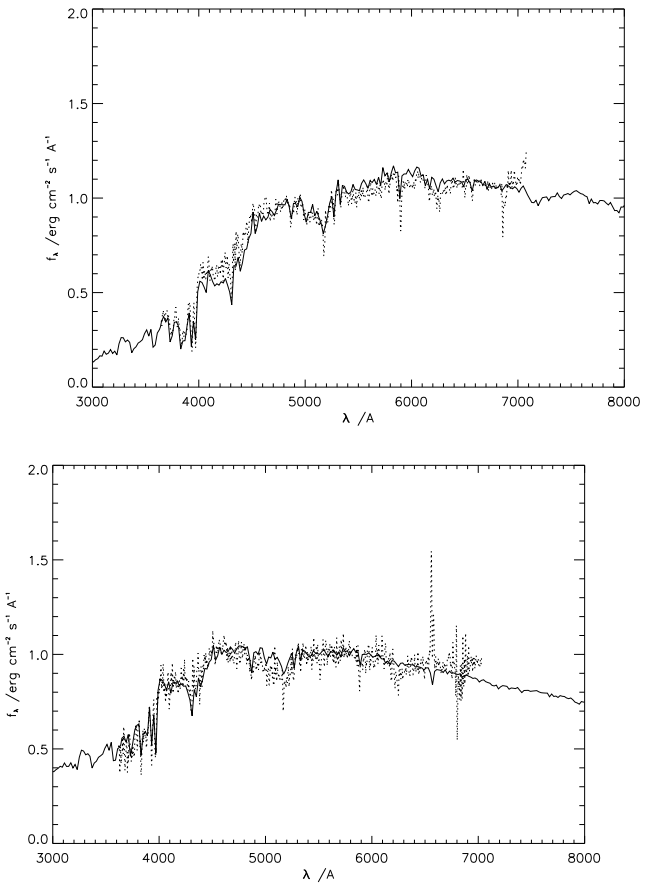

Fig. 2. Comparison of theoretical galaxy spectra (solid) with observations from Kennicutt (1992) (dotted). NGC 3379 (E0) with E - model of 11 Gyr (top panel), NGC 3147 with Sb - model of 12 Gyr (middle panel) and NGC 4449 with Sd - model of 8 Gyr (bottom panel).

ter agreement with observations than models with solar metallicity. After a Hubble time the chemically consistent method gives (B-V) values, depending on the star formation rate, between 0.2 and 0.5 mag bluer than that of the model with solar metallicity.

For another test of our models we compared our integrated galaxy spectra with observations from a sample of 90 nearby ($z \leq 0.03$) galaxies of various spectral types from Kennicutt (1992). The observed galaxy spectra cover a wavelength range from 3650 - 7000 Åand the spectral resolution varies from 5 Å to 25 Å, while our model spectra have a resolution of 20 Å in this range.

In Fig. 2 we compare some of Kennicutt's template spectra with our synthetic model spectra of the respective Hubble types. The model spectra are computed without gaseous emission lines. Fig. 2a) shows NGC 3379 (=E0 template) with our elliptical model, b) NGC 3147 (Sb) with our Sb-model and c) NGC 4449 an irregular galaxy (Sm/Im) which seems to be well described by the constant SFR of our Sd-model. The spectrum of NGC 3379 is fitted well by our 11 Gyr old E - model. Because the spectral energy distribution of ellipticals evolves strongly during the first 12 Gyr, the age of NGC 3379 can be restricted to a small range. The spectrum of a young elliptical declines at $\lambda \geq 6000$ Å, while the Balmer jump becomes higher in older E - galaxies because of the accumulation of low mass main - sequence stars and cold giants. NGC 3147 is well reproduced by a 12 Gyr old Sb - spectrum. Our Sd - models with an age of 8 -9 Gyr are suitable for the NGC 4449 spectrum. Because of a constant star formation rate the spectrum of an Sd - galaxy doesn't evolve very much, resulting in an age dating, that is less precise than for early type galaxies. The time dependent composition of the five stellar tracks produces the smooth evolution of the Sd spectrum.

Bruzual & Charlot (1993) and Bruzual (1995) produced solar metallicity models and fit the observed spectrum of NGC 3379 with a 13.8 Gyr old elliptical spectrum, that of NGC 3147 with an 8 Gyr old Sb - spectrum and that of NGC 4449 with a 1 Gyr young Sd - spectrum (constant star formation rate). This shows that the strong subsolar metallicity of late type galaxies leads to erroneously low ages when determined from a solar metallicity model.

For a more detailed description of our models see Möller (1995), where all colors are calculated from the U to K band, and the color evolution over a large redshift range, assuming a set of cosmological parameters, is compared to observations of high redshift galaxies.

4. Metallicity indicators in different wavelength regions

4.1. Evolution of ISM abundances

In Fig. 3 we show the enrichment of the ISM metallicity Z for the star formation histories ascribed to the different galaxy types. The horizontal lines mark the five metallicity regimes and delineate the critical ISM metallicities at which we change, for the newly born stars, from one set of stellar evolutionary tracks to another.

The metallicity of spiral galaxies increases steadily with time. The enrichment is faster and stronger for earlier spiral types because of their higher star formation rates. Owing to the very strong star formation in the first Gyr, the ISM abundance in ellipticals increases strongly up to 3 Gyr. At this time, virtually all of the gas is consumed by star formation and most of the massive stars have already died out. After that the lower mass stars begin dying in large numbers, increasing the total gas content but mainly giving back unenriched material. This accounts for the well-known dilution effect of the ISM in ellipticals. The strength of the dilution effect depends on the ratio of low mass stars to high mass stars given as by the IMF. While a dilution effect is clearly seen for a Scalo IMF, a Salpeter IMF with its lower ratio of low - to - high mass stars only causes a leveling - off of the ISM metallicity for $t \geq 3$

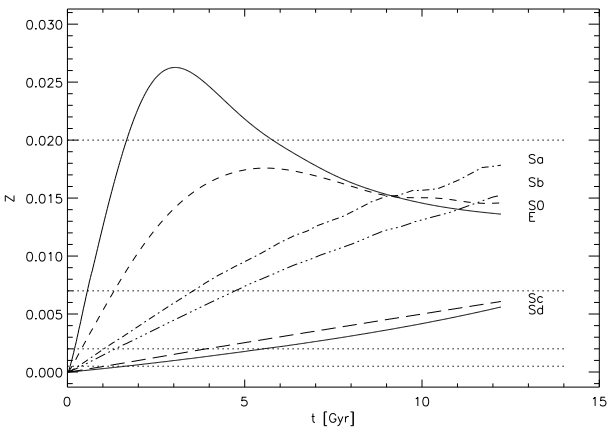

Fig. 3. Time evolution of ISM metallicity for various spectral types. The horizontal lines mark the five discrete metallicity regimes.

Gyr. Our model ISM abundances agree with observations (e.g. Zaritsky et al. 1994) for the various galaxy types. Because of their significantly subsolar metallicity, the effects of chemical enrichment will be more important and visible in the spectrophotometric appearance of late type galaxies. Except for the central regions of massive ellipticals, the average stellar metallicities in dwarf and normal ellipticals are expected to be subsolar as well.

4.2. Luminosity weighted stellar metallicities

As described above, a major problem with composite stellar populations is that the same broadband color can be produced by young metal - poor stars as well as by old metal - rich stars (e.g. O'Connell 1976, Arimoto & Yoshii 1987, Bica et al. 1988, Faber et al. 1995). It is likewise well known that the NIR is much less age dependent than the optical or the UV. For this and other reasons metal indices are investigated in the NIR (e.g. Frogel 1985, Terndrup et al. 1991, Lançon & Rocca - Volmerange 1992). We analyse the luminosity weighted stellar metallicities as a function of wavelength because their behaviour is important for the comparison of metal indices in different bands. Metallicities deduced from observations are always luminosity weighted, in contrast to mass-averaged metallicities of composite stellar populations (Matteucci 1994).

We use the following definition for our calculations of the luminosity weighted stellar metallicities:

$$Z_\lambda = a_1 \cdot Z_1 + a_2 \cdot Z_2 + a_3 \cdot Z_3 + a_4 \cdot Z_4 + a_5 \cdot Z_5 \qquad (1)$$

where $a_i := \frac{L_\lambda(Z_i)}{L_{\lambda tot}}$ is the relative contribution to the luminosity L_λ in the band λ from stars with metallicity Z_i.

This luminosity weighted stellar metallicity can differ greatly from a mass-weighted one. Arimoto & Yoshii (1987) and Matteucci & Tornambè (1987) have already shown that, in general, the luminosity averaged metallicity in visual light is smaller than the mass-weighted one, since metal poor giants dominate this wavelength region. It is worth noting that in simple stellar populations Z_λ is the same in all wavelengths and that differences in Z_λ can only be described by a chemically consistent evolutionary synthesis.

The evolution of the gas metallicity reflects the star formation history, but is not linearly correlated with the metallicity of the stellar population. ISM abundances are normally obtained from HII regions.

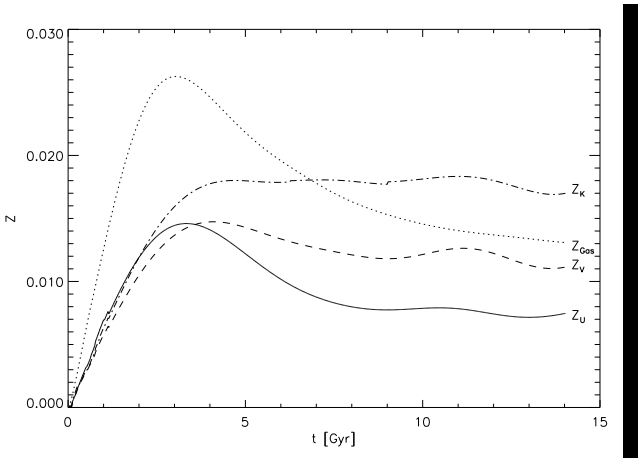

Fig. 4. Time evolution of luminosity weighted stellar metallicities Z_U(solid), Z_V(dashed) and Z_K(dash-dotted) and of ISM metallicity (dotted) for ellipticals.

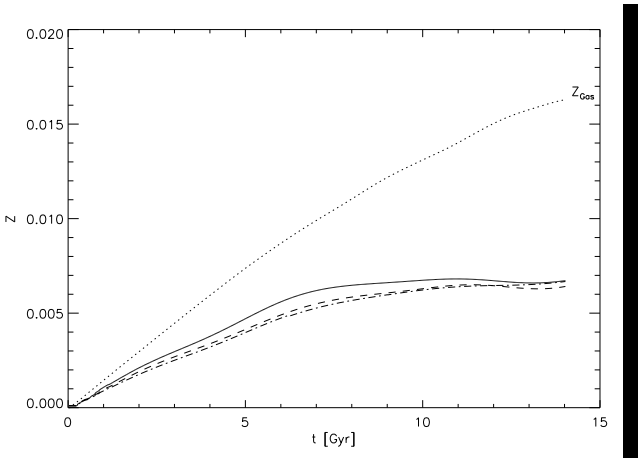

Fig. 5. Same as in Fig. 4, but for Sb - galaxies.

In Fig. 4 - 6 we compare the time evolution of ISM metallicities to the luminosity weighted stellar metallicities for galaxy types E, Sb and Sd. In ellipticals (Fig. 4) the enrichment of the metallicity is faster in the gas than in the stellar population. Like the ISM abundance, all stellar metallicities $Z_U ... Z_K$ increase during the first 3 - 4 Gyr. Only Z_U, which is dominated by massive young stars, decreases after a maximum, in a very similar manner to the

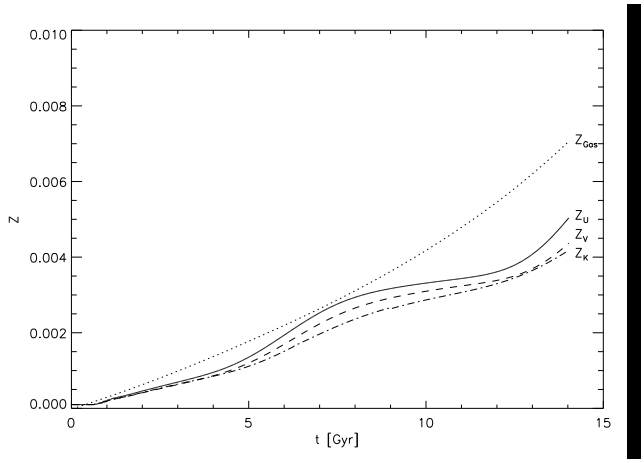

Fig. 6. Same as in Fig. 4, but for Sd - galaxies.

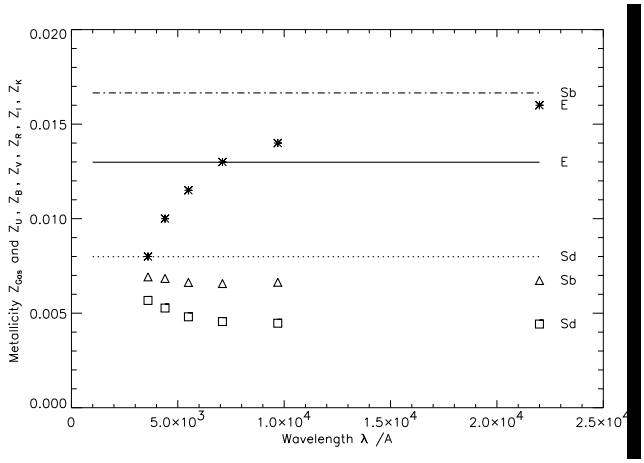

Fig. 7. Comparison of stellar metallicities Z_U, Z_B, Z_V, Z_R, Z_I, Z_K with gas metallicity (horizontal lines) after 15 Gyr for E (star), Sb (triangle) and Sd (box).

dilution in the gas. Any stars formed at times later than ∼4 Gyr will again have lower initial metallicities. Very different is the behaviour of Z_K which nearly stays at its maximum. Z_K mainly represents the average metallicity of cold, low - mass main sequence stars and red giants which give strong contributions to the luminosity in K. After 7 Gyr the gas metallicity decreases below the value of the stellar metallicity in K because of the above mentioned dilution effect. The mean mass - weighted stellar metallicity is lower than Z_K and obviously cannot exceed the gas abundance.

The stellar metallicities in Sb - spirals (Fig. 5) steadily increase with time. There is very little difference between luminosity weighted stellar metallicities at various wavelengths from optical to UV. Z_U through Z_K stay below the ISM metallicity by a factor of two throughout a Hubble time. For Sd type galaxies, with their star formation rate being constant in time, stellar metallicities from U through K are very similar and only differ slightly from the global ISM metallicities (Fig. 6).

Figs. 4,5 and 6 clearly show that stellar metallicity indicators at different wavelengths and HII - regions abundances have to be expected to give significantly different results. Our models quantify these differences and explicitly show how these depend on the SF history.

To analyse the characteristic differences, we show in Fig. 7 the luminosity weighted stellar metallicities $Z_U, Z_B, Z_V, Z_R, Z_I, Z_K$ and the ISM abundance for different galaxy types after 15 Gyr. Going from the U to the K band the trend for luminosity weighted stellar metallicities in ellipticals is just the inverse to that for spirals. Even within a single galaxy, metal abundances derived from different wavelength regions are predicted to differ by as much as a factor of two. The metal enrichment of the stars differs from that of the gas by a factor of two in Sb - galaxies, more than in any other type of galaxy (Möller et al. 1995). This explains the differences between both the metallicities and Galactic metallicity gradients derived from HII - region abundance studies and metallicities individually determined for samples of B-, G-, K- or M stars which emit their dominant light contributions at different wavelengths (Nissen 1995, Kilian et al. 1994, Edwardsson et al. 1993).

Table 2. Percentage luminosity contribution to the total luminosity $L_{tot}[10^9 L_\odot]$ in U, V, K bands from stellar subpopulations of different metallicities at 15 Gyr.

Z =	10^{-4}	10^{-3}	$4 \cdot 10^{-3}$	10^{-2}	$4 \cdot 10^{-2}$	L_{tot}
			E			
L_U	14.9	16.8	38.5	28.6	1.2	16.1
L_V	6.5	10.2	29.0	52.2	2.1	24.5
L_K	2.7	5.1	14.7	75.6	1.9	81.9
			Sb			
L_U	5.1	5.6	22.3	67.0	-	39.0
L_V	3.0	3.9	30.0	63.1	-	43.6
L_K	1.6	2.8	31.4	64.3	-	116.1
			Sd			
L_U	0.9	18.7	80.4	-	-	158.0
L_V	1.1	15.5	83.4	-	-	91.3
L_K	1.2	10.9	87.9	-	-	120.6

To further explain these results, we show in Table 2 the percentage luminosity contributions to the U, V, K filters from stellar subpopulations of different metallicities at an age of 15 Gyr. Column 7 contains, respectively, the total luminosity L_U, L_V, L_K in $[10^9 L_\odot]$. The dominant contribution to the K luminosity in ellipticals is from stars with metallicities of about 0.5 $Z_\odot$. This stellar subpopulation which accounts for 2/3 of the total light in K, represents at the same time, the bulk of the stellar mass

in normal ellipticals. The luminosity distribution in V is somewhat broader than in K, while the broadest metallicity distribution is found in U. The luminosity in U is mainly due to late forming massive stars with subsolar metallicities. The maximum of the metallicity distribution depends on wavelength, approximately $Z = 4 \cdot 10^{-3}$ in U and up to $Z = 4 \cdot 10^{-2}$ in the K band. Stars with $Z \sim 2Z_{\odot}$ do not significantly contribute to the integrated U, V and K light. While the metallicity distribution of stars contributing light to some band reaches a maximum and then declines towards the highest metallicities in each band for ellipticals, it shows a monotonic, though overall weaker, increase in spirals. There are characteristic differences between early and late type spirals. In Sb - galaxies, $L_K \geq L_U, L_V$ for every metallicity subpopulation except 10^{-4}, while in Sds, $L_U \geq L_V, L_K$ for all metallicities. As expected from Fig. 1, the maximum metallicity reached by stars is 0.5 $Z_{\odot}$ in an Sb - spiral and $Z = 4 \cdot 10^{-3}$ in an Sd - galaxy.

4.3. Discussion

In 1988, Bica et al. already presented an analysis of the V light contributions of different metallicity components in nuclei and entire galaxies of various star formation histories. To do this, they combined star cluster population synthesis with $M/L_V(t)$ from Arimoto & Yoshii's evolutionary synthesis. Using a very flat IMF (x= 0.95), their model results in a stronger enrichment and consequently gives stronger V light contributions of high metallicity components as compared to our model.

We want to recall that, though it's not possible in our model to constrain the IMF and the SF histories independently of each other, our combination of a uniform IMF with empirical SF histories as given in Table 1, yields ISM abundances that agree with those observed by Zaritsky et al. (1994) in a large sample of galaxies.

To conclude, we find that the dominant light contributions to the various bands in global galaxy models are from stars of $\sim 0.5Z_{\odot}$ metallicity for normal gEs to Sb galaxies, while in Sd galaxies it comes from stars of lower metallicity. The situation may of course be different in the nuclei or bulges of galaxies, in dwarf ellipticals and cD galaxies, for which our simple one-zone, closed box models do not apply.

5. Metal Indices

5.1. Time evolution and relations with [Fe/H]$_*$

Integrated stellar metallicities of galaxies are generally determined from observations of characteristic stellar absorption features (e.g. Mg_2, Mgb, iron lines, TiO bands, etc.). Unless reliable emission line subtraction can be performed, these metal indices can only be measured from emission free spectra of early type galaxies. As explained in Sec. 2.2, we calculate the time evolution of a series of stellar metallicity indicators for our model galaxies. For

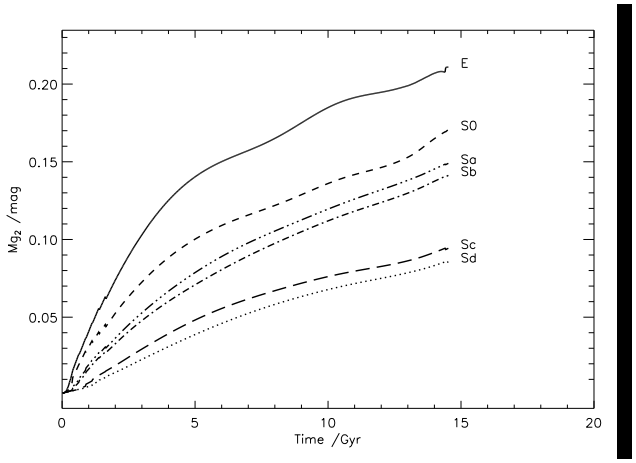

Fig. 8. Time evolution of Mg_2 for galaxy models of different spectral types.

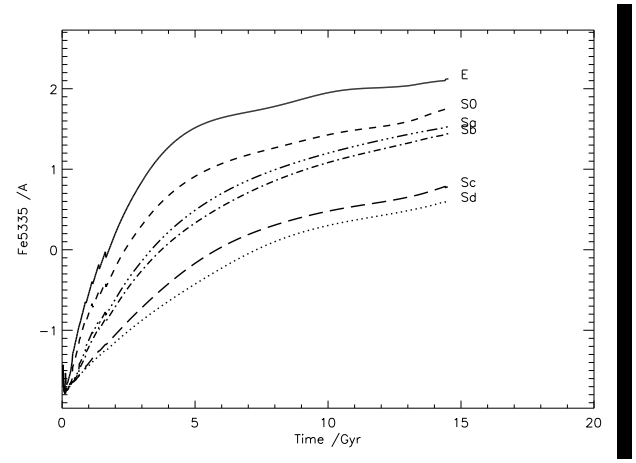

Fig. 9. Time evolution of Fe5335 for galaxy models of different spectral types.

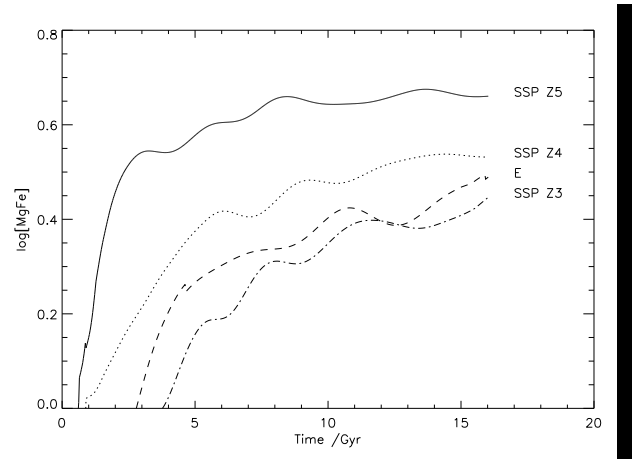

Fig. 10. Time evolution of stellar index [MgFe] for an E-galaxy model (dashed) and for three SSPs with Z3=$4 \cdot 10^{-3}$ (dot-dashed), Z4=10^{-2} (dotted) and Z5=$4 \cdot 10^{-2}$ (solid). The range of observations (Gonzales 1993) is given by the perpendicular line.

the case of early type galaxies these can be directly compared to observations.

We show the time evolution of Mg_2 and Fe5335 in Figs 8 and 9 for the Hubble sequence of galaxies from E to Sd. As expected, the stellar magnesium and iron indices increase continuously for all galaxy types. These indices rise faster and reach higher values in ellipticals, although their final gas metallicity is lower than in early type spirals after a Hubble time. The metallicity indices we analyse represent the metallicity of the stellar population which dominates the light in the V band. The time evolution of these indices reflects that of Z_V because both indices lie in the V filter, but their metallicity dependence is different, as already shown by Worthey (1994). He calculates a Z sensitive parameter, which is the ratio of the percentage change in age to the percentage change in Z. This parameter is higher for the iron indices than for the magnesium indices, i.e. the iron indices as defined by Gorgas are more Z sensitive. The iron index increases faster than the Mg_2 index in early galaxy types. It should be noted that the rate of time evolution is different for different indices and evolutionary epochs, as well as for broad band colors. For simple stellar populations, such as star clusters, Fritze -v. Alvensleben & Burkert (1995) have shown that this effect allows to better disentangle age and metallicity, particular at early stages. For a stellar metallicity confirmed by spectroscopic observations, ages derived from the observed Fe5270 index agree well with ages derived from the broad band color (V-I).

It is clear that for a composite stellar system, e.g. a galaxy, with its different metallicity and age subpopulations, disentangling both effects becomes more difficult.

The theoretical Mg_2 and iron indices in our one - zone model galaxies are expected to be a lower limit to observed values because these observations typically refer to the central parts of galaxies. Moreover, in ellipticals the Mg_2 index is higher in mass rich galaxies, as expressed in the well known luminosity - metallicity relation, while our models refer to a mean elliptical galaxy luminosity of $M_B \sim 20.5$ at an age of 15 Gyr. To reduce this shortcoming of the one - zone model we compare it with indices determined from large aperture spectra of galaxies. Another way of testing our model is to simulate the central region of early type galaxies with SSPs of various metallicities.

5.2. Comparison with observations of Mg_2 and [MgFe]

The Mg_2 observations on globular clusters from Brodie & Huchra (1990) are well reproduced with our Single-Burst - models (cf. Einsel et al. 1995). These observed Mg_2 values of globular clusters in the regime of subsolar metallicities are in the range of $0.05 \leq Mg_2$ [mag] ≤ 0.20. Calibrations for Mg_2 vs. stellar $[Fe/H]_*$ are given by Burstein et al. (1984) as derived from observations of globular clusters and by Buzzoni et al. (1992) as derived from their evolutionary synthesis models. The work of Matteucci & collaborators (1987 ff) has shown that the iron abundance evolution should not be expected to directly correspond with magnesium because of SNI contributions. Instead of the usual Mg_2 vs. $[Fe/H]_*$ relation, a calibration between the mean luminosity weighted stellar metallicity and various indices might be more useful because both can be observed. In our notation, a calibration of Mg_2 vs $[Fe/H]_*$ for elliptical galaxies could be expressed as a relation between Mg_2 and Z_V. From the monotonic increase of Mg_2 with time (Fig. 8) and the enrichment and subsequent dilution behaviour of $Z_V(t)$ (Fig. 4), it is clear that no unique relation between Mg_2 and Z_V is obtained for our composite metallicity elliptical galaxy model. Observations of stellar metallicities in different wavelength regions might even provide information about the SF history of the galaxy.

Fig. 10 shows the time evolution of the stellar index [MgFe]. In this figure we compare the SSPs for three metallicities with the chemically consistent model of an elliptical galaxy. As expected from Figs. 8 and 9 the [MgFe] evolution of our composite elliptical galaxy model remains below that of a half solar SSP model over a Hubble time. Observations of [MgFe] by Gonzales (1993) of the central regions of elliptical galaxies, i.e. within Re/8 and Re/2, where Re is the effective radius (see also Bressan et al. 1995), lie between $0.4 \leq$ log[MgFe] ≤ 0.6, with the bulk of the Re/2 data at $\sim$0.53. The evolution of [MgFe] from the SSPs with $Z=10^{-2}$ and $Z=2Z_\odot$ fit these data well, while as expected, our global elliptical model with [MgFe] ~ 0.48 only gives a lower limit to the observed central [MgFe].

5.3. Relations between indices and ISM abundances

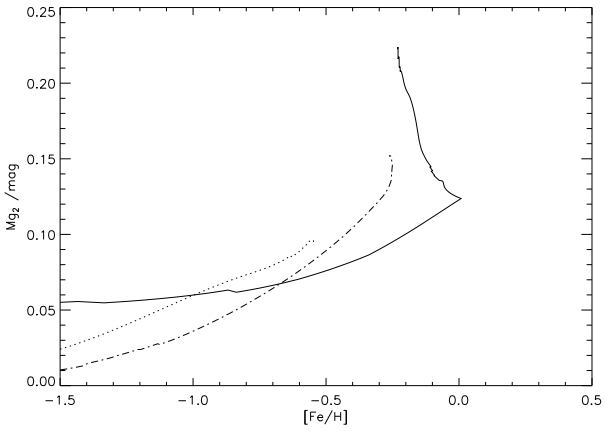

Fig. 11. Stellar index Mg_2 versus $[Fe/H]_{ISM}$. The solid curve shows the time evolution for E - galaxies, the dot-dashed that for Sb - galaxies and the dotted that for Sd - galaxies.

It is interesting to find a relation between stellar indices and the ISM metallicity despite the fact that in the past, stellar indices have generally been measured from

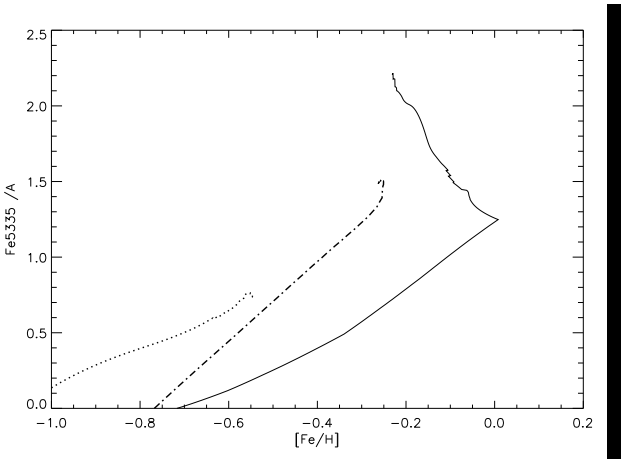

Fig. 12. Time evolution of stellar index Fe5335 vs. $[Fe/H]_{ISM}$ for ellipticals (solid), Sb - galaxies (dot-dashed) and Sd - galaxies (dotted).

elliptical galaxies while ISM abundances were determined from HII - region observations in spiral galaxies.

Cold molecular gas has now been found in several ellipticals (cf. e.g. Lees et al. 1991) and abundance determinations from sub-mm lines may be possible in the near future. X-ray observations of the hot coronae of massive ellipticals has already provided abundances for the diluted hot gas, which is possibly being blown out of the galaxies (Arimoto 1995). To determine the origin of this gas, a comparison with model ISM properties may be useful, though in this case a generalization of our simple closed-box model would be required.

QSO absorption line observations and optical identification of absorbers point to large gaseous halos containing sufficient amounts of magnesium and carbon to overcome the lower equivalent width thresholds of these observations around early and possibly even late type galaxies (see Dickinson 1995, Tytler 1995 for a recent review). These observations will soon offer a unique opportunity to model at the same time the spectral signature of the galaxy, including stellar absorption features **and** its ISM abundances.

Here, we will use our chemically consistent photometric evolutionary model, together with a detailed description of the iron enrichment in the ISM to derive relations of stellar Mg_2 and Fe5335 with $[Fe/H]_{ISM}$ as a function of star formation history. We can then study how these relations evolve as a function of galaxy age. We thus obtain theoretical relations between metal indices and gas metallicities, by modelling the enrichment of ^{56}Fe.

The difference between the evolution of ^{56}Fe and ^{24}Mg is that the dilution of ^{56}Fe is not as strong as that of ^{24}Mg due to the continuing iron - enrichment from SNeI. The evolution of the global gas metallicity Z is similar to that of ^{16}O and ^{24}Mg because these typical SNII products make up the bulk of the heavy elements.

The time evolution of the relation between stellar indices Mg_2, $Fe5335$ and gas metallicity given in terms of $[Fe/H]_{ISM}$ is presented in Figs 11 and 12 for E, Sb and Sd galaxies. While the values of both the stellar indices and $[Fe/H]_{ISM}$ in spirals increase continuously with time (Fig. 11, 12), the relation for ellipticals is not unique. This is because of the maximum and later dilution in the ISM of $[Fe/H]_{ISM}$ and the continuous increase of Mg_2 (Fig. 8). While the lower branch of the evolution for ellipticals belongs to very early phases ($\leq$ 3 Gyr), the upper one, which is roughly perpendicular to the relation for spirals, gives the evolution after the ISM abundance maximum.

These calibrations between stellar metal indices and $[Fe/H]_{ISM}$ are obviously a first approximation and have to be extended to also include dynamical effects, such as e.g. mass loss through SN-driven galactic winds or the formation of abundance gradients. Dropping our simplifying one - zone, closed box assumption would result in a metallicity gradient and imply metallicities that will probably be lower in the outer part and higher in the central regions as compared to our overall metallicity. In the central regions the metallicity may even increase to a few times solar, so that additional stellar tracks of higher metallicity become necessary. All this, however, is beyond the scope of the present paper.

6. Summary

Using our chemically consistent evolutionary method, which follows the enrichment of metallicity in the ISM and in successive generations of stars, we are able to reproduce the observed colors for different spectral types of galaxies. We obtain good agreement of our synthetic galaxy spectra at ages of 11, 12 and 8 Gyr for E -, Sb - and Sd - model galaxies with Kennicutt's observed templates. Our model ISM abundances also agree with Zaritzky's observations of various spiral types.

We analyse the evolution of and relations between different measurements of the metallicity: abundances of heavy elements in the ISM, luminosity weighted stellar metallicities in different wavelength bands, and various stellar absorption indices. We study the influence of the star formation history on luminosity weighted stellar metallicities and indices.

Important differences are found between luminosity weighted stellar metallicities at different wavelengths. For example in ellipticals, the stellar metallicity seen in the K - band is predicted to be higher by a factor of two than that seen in U. Going from the U to the K band the trend for luminosity weighted stellar metallicities in ellipticals is just the inverse to that for spirals, i.e. in spiral type galaxies the luminosity weighted stellar metallicity is higher in U than in V and K. For the Sb model the discrepancy between stellar and ISM abundances is larger than in the E or Sd model. The ISM metallicity of our Sb model is a factor of two higher than the luminosity weighted stellar metallicity in any wavelength region.

We analyse the luminosity contributions to various filters from stellar subpopulations of different metallicities for different spectral types of galaxies. While the metallicity distribution of stars contributing light to a passband reaches a maximum at $Z \sim 0.5Z_{\odot}$ and then declines towards the highest metallicities at all wavelength for ellipticals, it shows a monotonic, though overall weaker, increase in spirals. In addition, the maximum of the metallicity distribution in ellipticals depends on wavelength. At higher metallicity it is at shorter wavelength. Therefore, knowing the metallicity distribution allows one to constrain the age distribution for a known SF history in composite stellar populations.

We show for spectral types from E to Sd how the time evolution of the stellar metallicity indices Mg_2, Fe5335 and [MgFe] depend on the SF history. These indices increase continuously with time, with the iron index growing the fastest, which reflects the fact that it is more sensitive to metal enrichment than Mg_2. Although the stellar metal indices Mg_2 and Fe5335 lie in the V band, there is no unique relation with the luminosity weighted stellar metallicity Z_V, because Z_V reaches a maximum and is subsequently diluted.

We also calculate simple stellar populations for various metallicities and compare their [MgFe] time evolution with that of the chemically consistent model and observations from the central regions of ellipticals (Gonzales 1993). Our simple stellar populations with $Z=2Z_{\odot}$ and $Z=0.5Z_{\odot}$ fit well the observed central [MgFe], while our global E model as expected gives a lower limit.

Our models also allow one to study stellar features together with the evolution of ISM abundances, e.g. $[Fe/H]_{ISM}$. We present theoretical relations between Mg_2 and Fe5335 vs $[Fe/H]_{ISM}$ that will be useful for a consistent chemical and spectral interpretation of optically identified QSO absorbers.

While in our elliptical model the enrichment of the ISM does not directly correlate in a unique way throughout an entire Hubble time with that of the stellar population, we find a linear relation between stellar and ISM metallicity in spiral galaxy models.

Acknowledgements. We are grateful to Robert C. Kennicutt, Jr. for sending us his atlas of template galaxy spectra. We are also indebted to Gustavo Bruzual for providing us Kurucz's stellar atmosphere spectra. We thank our referee, Danielle Alloin, for very useful comments. C. S. M. and U. F.- v.A. acknowledge financial support from the Deutsche Forschungsgemeinschaft under grants Fr 325/36-1 and Fr 916/2-1. The computations were carried out on a HP - Workstationcluster in the Universitätssternwarte.

References

Arimoto, N., Yoshii, Y. 1986, A&A, **164**, 260
Arimoto, N., Yoshii, Y. 1987, A&A, **173**, 23
Arimoto, N. 1995, in *From Stars to Galaxies*, International Conference, in press
Bahcall, J.N., Flynn, C., Gould, A. 1992, ApJ, **389**, 234
Bessel, M.S., Brett, J.M. 1988, PASP, **100**, 1134
Bica, E., Alloin, D. 1986, A&A, **162**, 21
Bica, E., Alloin, D. 1987, A&A SS, **70**, 281
Bica, E. 1988, A&A, **195**, 76
Bica, E., Arimoto, N., Alloin, D. 1988, A&A, **202**, 8
Bressan, A., Chiosi, C., Tantalo, R. 1995, A&A, in press
Brodie, J.P., Huchra, J.P. 1990, ApJ **362**, 503
Bruzual A., G. 1993, in *The enviroment and Evolution of Galaxies,* eds. Shull, J.M., Thronson, H.A., Kluwer Academic Puplishers, p.91
Bruzual A., G., Charlot, S. 1993, ApJ **405**, 538
Burstein, D., Faber, S.M., Gaskell, C.M., Krumm, N. 1984, ApJ **287**, 586
Buzzoni, A., Gariboldi, G., Mantegazza, L. 1992, AJ **103**, 1814
de Vaucouleurs, G., de Vaucouleurs, A., Corwin, H.G., Buta, R.J., Paturel, G., Fouqué, P. 1991, in *Third Reference Catalogue of Bright Galaxies,* Springer Verlag
Dickinson, M. 1995, in *New Light on Galaxy Evolution*, IAU Symposium 171, in press
Einsel, Ch. 1992, Diploma Thesis, University of Göttingen
Einsel, Ch., Fritze - v. Alvensleben, U., Krüger, H., Fricke, K.J. 1995, A&A **296**, 347
Edwardsson, B., Andersen, J., Gustafsson, G., Lambert, D.L., Nissen, P.E., Tomkin, J. 1993, A&A **275**, 101
Faber, S.M., Tracer, S.C., Gonzalez, J.J., Worthey, G. 1995, in *Stellar Populations,* IAU Symp. # 164, eds. van der Kruit, P.C., Gilmore, G., Kluwer, Dordrecht, p.249
Fritze - v. Alvensleben, U. 1989, PhD Thesis, University of Göttingen
Fritze - v. Alvensleben, U., Gerhard, O.E. 1994, A&A **285**, 751
Fritze - v. Alvensleben, U., Burkert, A. 1995, A&A **300**, 58
Frogel, J.A. 1985, ApJ **298**, 528
Gonzales, J.J. 1993, Ph.D. Thesis, Univ. California, Santa Cruz
Gorgas, J., Faber, S.M., Burstein, D., Gonzalez, J.J., Courteau, S., Prosser, C. 1993, ApJS **86**, 153
Green, E.M., Demarque, P., King, C.R. 1987, in *The Revised Yale Isochrones and Luminosity Functions,* Yale Univ. Obs.
Guiderdoni, B., Rocca - Volmerange, B. 1987, A&A **186**, 1
Gunn, J.E., Stryker, L.L. 1983, A&A SS **52**, 121
Kennicutt, R.C. 1992, ApJ **388**, 310
Kilian, J., Montenbruck, O., Nissen, P.E. 1994, A&A **284**, 437
Krüger, H., Fritze - v. Alvensleben, U., Loose H.-H. 1995, A&A **303**, 41

Kurucz, R.L. 1992, in *The Stellar Populations of Galaxies,* IAU Symp. # 149, eds. Barbury, B., Renzini, A., Kluwer, Dordrecht, p.225
Lançon, A., Rocca - Volmerange, B. 1992, A&A **96**,593
Lees, J.F., Knapp, G.R., Rupen, M.P., Phillips, T.G. 1991, ApJ **379**, 177
Matteucci, F., Tornambè, A. 1987, A&A **185**, 51
Matteucci, F., Ferrini, F., Pardi, C., Penco, U. 1991, in *Chemical and Dynamical Evolution of Galaxies,* ETS, eds. Ferrini, F., p.577
Matteucci, F. 1994, A&A **288**, 57
Möller, C.S. 1995, Diploma Thesis, University of Göttingen
Möller, C.S., Fritze - v. Alvensleben, U., Fricke, K.J. 1995, in *Stellar Populations,* IAU Symp. # 164, eds. van der Kruit, P.C., Gilmore, G., Kluwer, Dordrecht, p.426
Nissen, P.E. 1995, in *Stellar Populations,* IAU Symp. # 164, eds. van der Kruit, P.C., Gilmore, G., Kluwer, Dordrecht, p.109
O'Connell, R.W. 1976, ApJ **206**, 370
Sandage, A. 1986, A&A **161**, 89
Scalo, J.M. 1986, Fundam. Cosm. Phys. **11**, 1
Taylor, B.J., Johnson, S.B., Joner, M.D. 1987, AJ **93**, 1253
Terndrup, D.M., Frogel, J.A., Whitford, A.E. 1991, ApJ **378**, 742
Tinsley, B.M. 1972, A&A **20**, 383
Tytler, D. 1995, in *New Light on Galaxy Evolution*, IAU Symposium 171, in press
Worthey, G. 1994, ApJS **95**, 107
Worthey, G., Faber, S.M., Gonzales, J.J., Burstein, D. 1994, ApJS **94**, 687
Wu *et al.* (eds.) 1983, IUE Ultrav. Spektral Atlas, NASA No. 22
Zaritsky, D., Kennicutt, R.C., Huchra, J.P. 1994, ApJ **420**, 87